Two and three-parameter isothermal modeling for adsorption of Crystal Violet dye onto Natural Illitic Clay: Nonlinear regression analysis

Otheman Amrhar*, Hakima Nassali and Mohamed S. Elyoubi

Laboratory of the Engineering of Materials and Environment, Faculty of sciences, IbnTofail University, Kenitra, Morroco

_____

ABSTRACT

In this study, the adsorption of a cationic dye, Crystal Violet (CV), from aqueous solution onto Natural Illitic clay (NIC) has been studied in batch system and the equilibrium isotherms were determined. The adsorbent has been characterized by chemical analyses, XRD and FTIR. Four two-parameter isotherm models namely Langmuir, Freundlich, Dubinin–Radushkevich and Temkin, and four three-parameter isotherm models namely Redlich-Peterson, Sips, Khan and Toth were used to analyse the experimental data. In order to determine the best fit isotherm, five nonlinear error functions namely, Nonlinear Chi-square test (X^2), Sum of the Squares of the Errors (SSE), Average Relative Error (ARE), Sum of the Absolute Errors (EABS), Hybrid Fractional Error Function (HYBRID), were used to evaluate the data. The error analysis demonstrated that the Sips isotherm model has better described the CV adsorption data onto NIC. Furthermore, the type of adsorption was determined from isotherm parameters, and it was concluded that the physic-sorption is the appropriate mechanism adsorption to CV onto NIC.

Key words: Adsorption, Crystal Violet, Natural Illitic Clay, equilibrium isotherm, error analysis.

_____

INTRODUCTION

The textile industries discharge enormous amounts of colored wastewater. The dyes contained in this wastewater are toxic, carcinogenic and resistant to degradation, which can cause the problems to the environment and to the living beings. So, it is necessary to eliminate dyes from wastewater before it is discharged. A wide range of methods have been developed for remove of synthetic dyes from wastewater, including coagulation[1], ozonation[2], membrane separation[3], electrochemical technique[4], ultrasonic technique[5], and adsorption[6]. This last technique is gaining more attention because of its relatively low cost, high availability, high performance, and its ability to treat the wastewater in different concentrations. Many adsorbents are widely used such as activated carbon[7], chitosan[8], and clay[9–11]. The Modeling of adsorption isotherm data is important for predicting the adsorption performance and to design the adsorption system. Two-parameter isotherm models such as: Langmuir[12], Freundlich[13], Dubinin–Radushkevich[14], Temkin[15], and three-parameter isotherm models such as: Redlich-Peterson[16], Sips[17], Khan[18] and Toth[19]can be used for modeling adsorption isotherm data.

Generally, to determine the isotherm constants for an adsorption system, two regression methods are available. The linear regression method consists in converting the isotherm equation to a linear form, then, the fitting of the isotherm equation (in linear form) to the experimental data well be made. Thus, the nonlinear regression method is based on fitting the isotherm equation in its nonlinear form to the experimental data. The search for the best fit adsorption isotherm using the linear regression method is the widely used technic to determine the best fitting model and to evaluate the model parameters. However, depending on the way of the isotherm equation linearization, the distribution of error changes either the worst or the best[20]. Additionally, the linear regression method is not always a good choice to apply for isotherms with more than two parameters. So, the method of nonlinear regression is used by several researchers to determine the best fitting isotherm model[20–23]. It is based on the minimization of error

_____

distribution between the experimental adsorption data and the predicted isotherm model. It has an advantage that the error distribution does not get altered as in linear regression method because all isotherm parameters are fixed in the same axis.

Several error functions are used to evaluate the isotherm data by nonlinear regression method. The most common error functions used are: The Nonlinear Chi-square test (X^2), The Sum of the Squares of the Errors (SSE), The Average Relative Error (ARE), The Sum of the Absolute Errors (EABS), The Hybrid Fractional Error Function (HYBRID)[22–24].

Crystal violet, also namely gentian violet, belongs to the class of Triarylmethane dyes. Its IUPAC name is *N-[4-[bis[4-dimethylamino)-phenyl]-methylene]-2,5-cyclohexadien-1-ylidine]-N-methylmethanaminium chloride*, with molecular formula *$C_{25}N_3H_{30}Cl$*, and *407,979 g.mol⁻¹* as a molecular weight. The Crystal Violet is used in laboratory as a PH indicator and as a bacteriostatic agent. It is also used as a dye for textiles, and in paints and printing ink. It can cause several health problems such as moderate eye irritation, cancer, and it is harmful by ingestion, inhalation and through skin contact[25].

In this work, the isotherm models mentioned above were used, to represent the adsorption isotherm data of a cationic dye, Crystal Violet (CV), onto Natural Illitic clay (NIC). The nonlinear regression method using error analysis was adopted to predict the optimum adsorption isotherm model, and also, to obtain the isotherm parameters to characterize the adsorption nature of CV onto NIC. Furthermore, the characterizations of Natural Illitic clay before and after adsorption have been donned by using XRD analysis and FTIR spectroscopy.

EXPERIMENTAL SECTION

Materials
The sample of Natural Illitic Clay (NIC) was collected from a deposit in the *KHEMISSET* region in *MOROCCO*. It was crushed, sieved through a standard ASTM sieve ($< 56\mu m$) to obtain the lower fractions, and then, dried in an oven at *110 ° C* during *2 hours* for the adsorption tests. The chemical composition of the NIC was obtained by Spectrometer dispersion wavelength (WD- XRF) - Type Axios-. The X-ray diffraction (XRD) analysis was determined using XPERT-PRO diffractometer, while The Fourier Transform Infrared (FTIR) spectrum was obtained by using the Fourier transform infrared Spectrophotometer (*Tenser 27 spectrometer*) in the range of *$400–4000cm^{-1}$*. The dye used in this study is the Crystal Violet (CV). It was obtained from *LaboChemie, INDIA*, and it was used as received. Its structure has been shown in **Figure 1**.

Figure 1: The Chemical structure of Crystal Violet (CV)

The dye stock solution was prepared by dissolving *0.407g* of CV in one liter of distilled water, and the required concentration of the working dye solution was prepared by diluting the stock solution with distilled water.

Batch adsorption experiments
A batch adsorption method was used to study the adsorption of Crystal Violet (CV) dye onto the Natural Illitic Clay (NIC). The initial CV dye concentration was varied in range of *5-30 mg.L⁻¹*, and for each initial dye concentration, the experiment was conducted by mixing twenty milligrams of NIC to twenty milliliter of CV solution, at natural solution PH, on a mechanical shaker at *600 rpm* during *60 min*. After separation of the solid phase and the liquid phase, the remaining concentration of CV in the filtrate was determined by using *SP 2000 UV* spectrophotometer. The amount of adsorbed CV dye onto NIC was calculated using the following equation

$$Q_e = \frac{(C_i - C_e)\,\mathrm{V}}{m}$$

Where $Q_e(mg.g^{-1})$ is the equilibrium adsorption capacity of Crystal Violet adsorbed on unit mass of Natural Illitic Clay, $C_i(mg.L^{-1})$ and $C_e(mg.L^{-1})$ are the initial Crystal Violet concentration and the Crystal Violet concentration at equilibrium, respectively, *V(L)* is the volume of the Crystal Violet solution, and *m(g)* is the weight of Natural Illitic Clay.

Equilibrium isotherms

In general, the adsorption isotherm indicates how the quantity of molecules are distributed between the liquid phase and the solid phase when the adsorption processes reach balance[26]. It gives important information about the main mechanisms involved in the removal of adsorbate by adsorbent. In this study, the equilibrium adsorption of CV onto NIC was studied as a function of CV concentration *(5-30 mg.L⁻¹),* andthe isotherm equilibrium data were analyzed using eight different adsorption isotherm models: Four two-parameter isotherm models as: Langmuir, Freundlich, Dubinin–Radushkevich (D-R), and Temkin, and four three-parameter isotherm models as: Redlich-Peterson, Sips, Khan and Toth.

- **Two-parameter isotherm models**

Four two-parameter isotherm models were used to study the present adsorption system, as: Langmuir, Freundlich, Dubinin–Radushkevich (D-R), and Temkin. The Langmuir isotherm theory assumes the monolayer coverage of adsorbate over a homogeneous adsorbent surface where all adsorption sites are found to be identical and energetically equivalent [12]. Whereas, the Freundlich isotherm model is valid for the multilayer adsorption on a heterogeneous adsorbent surface and predicts that the adsorbate concentration on the adsorbent will increase with the increasing of the adsorbate concentration in the solution[13]. Apart from these, the D-R model is applied to distinguish between the physical and chemical adsorptions[14], and lastly, the Temkin isotherm model assumes that the decrease in the heat of adsorption is linear and the adsorption is characterized by a uniform distribution of binding energies[15] .

The Langmuir, Frendlich, D-R and Temkin equations are presented in **Table 1**.

Table 1: The Two-parameter isotherm models used in this study

Isotherm	Nonlinear form	Parameters	Ref.
Langmuir	$Q_e = \dfrac{Q_{max} K_L C_e}{1 + K_L C_e}$	$*K_L$(the Langmuir isotherm constant, $L.mg^{-1}$)$*Q_{max}$ (the maximum amount of adsorbed dye per an unit weight of adsorbent, $mg.g^{-1}$)	[12]
Freundlich	$Q_e = K_f C_e^{1/n}$	$*K_f$(the Frendlich isotherm constant, $L.mg^{-1}$) $*1/n$ (the heterogeneity factor , limited between 0 and 1)	[13]
D-R	$Q_e = Q_{max} exp\left(-B_D \left[RT\,ln\left(1+1/Ce\right)\right]^2\right)$	$*B_D$ (related to the sorption energy E by means of the relationship: $E=1/(2B_D)^{0.5}$, $mol^2.Kj^{-2}$)	[14]
Temkin	$Q_e = \dfrac{RT}{b} Ln(K_T C_e)$	$*b(=RT/B$ related to the heat of adsorption , $J.mol^{-1}$) $*K_T$ (the Temkin equilibrium constant corresponding to the maximum binding energy, $L.g^{-1}$)	[15]

Where $Q_e(mg.g^{-1})$ and $C_e(mg.L^{-1})$ are the solid phase concentration and the liquid phase concentration of adsorbate at equilibrium, respectively.

- **Three-parameter isotherm models**

The Redlich-Peterson, the Sips, the Khan and the Toth isotherm models were used as three-parameter isotherm models in the present investigation. The Redlich– Peterson isotherm model[16] may be used to represent an adsorption equilibrium over a wide concentration range. It combines some elements from both the Langmuir and the Freundlich equations, and consequently, it can be employed either in heterogeneous or homogenous systems. Whereas the Sips isotherm model[17] is a combined form of Langmuir and Freundlich models: At a low adsorbate concentration, this model is reduced effectively to the Freundlich isotherm and did not obey to the Henry's law, and at high adsorbate concentrations, it predicts a monolayer sorption capacity which is characteristic of the Langmuir isotherm[27]. Apart from, the Khan isotherm model[18] suggest a generalized isotherm for the pure solutions, and

_____

lastly, the Toth isotherm model[**19**] is another isotherm that has three parameters Q_t, K_t and $1/t$, and useful in describing heterogeneous adsorption system, which satisfying both low and high-end boundary of the concentration. The Redlich-Peterson, Sips, Khan and Toth isotherm models are summarized in **Table2**.

Table 2: The Three -parameter isotherm models used in this study.

Isotherm	Nonlinear form		Ref.
Redlich-Peterson	$Q_e = \dfrac{AC_e}{1 + BC_e{}^g}$	*A (the Redlisch–Peterson isotherm constants, $L.g^{-1}$) *B (the Redlisch–Peterson isotherm constants, $L.mg^{-1}$) *g (an exponent which lies between 0 and 1)	[**16**]
Sips	$Qe = \dfrac{Q_s K_S C_e{}^{1/n}}{\left(1 + K_S C_e{}^{1/n}\right)}$	*Q_s (the Sips maximum adsorption capacity, $mg.g^{-1}$) *K_S (the Sips model isotherm constant, $L.g^{-1}$) *$1/n$ (the Sips model exponent)	[**17,27**]
Khan	$Qe = \dfrac{Q_{max} b_k C_e}{\left(1 + b_k C_e\right)^{a_k}}$	*a_k (the Khan model exponent) *b_k (the Khan model constant) *Q_k(the Khan maximum adsorption capacity, $mg.g^{-1}$)	[**18,27**]
Toth	$Qe = \dfrac{Q_t K_t C_e}{\left(1 + (K_t C_e)^t\right)^{1/t}}$	*Q_t (the Toth maximum adsorption capacity, $mg.g^{-1}$) *K_t (the Toth model isotherm constant) *$1/t$ (the Toth model exponent)	[**19,26**]

Error functions

To evaluate the fit of the above mentioned theoretical models to the experimental data, the nonlinear optimization method has been applied. This optimization procedure requires an error function to be defined in order to be able to evaluate the fit of the isotherm model to the experimental equilibrium data. In this work, five different error functions were examined by minimizing the respective error function across the concentration range studied, using the *"SOLVER ADD-IN"* with Microsoft's spread sheet. The error functions used in this study are presented in **Table 3**.

Table 3:The error functions used in this study

Error function	Definition	Ref.
The Sum of the Squares of the Errors (SSE)	$\displaystyle\sum_{i=1}^{n} \left(q_{e\,cal} - q_{e\,exp}\right)_i^2$	[24]
The average relative error (ARE)	$\dfrac{100}{n} \displaystyle\sum_{i=1}^{n} \left| \dfrac{q_{e\,cal} - q_{e\,exp}}{q_{e\,exp}} \right|_i$	[24]
The sum of the absolute errors (EABS)	$\displaystyle\sum_{i=1}^{n} \left| q_{e\,cal} - q_{e\,exp} \right|_i$	[24]
Nonlinear chi-square test (X^2)	$\displaystyle\sum_{i=1}^{n} \dfrac{\left(q_{e\,exp} - q_{e\,cal}\right)_i^2}{q_{e\,cal}}$	[22]
The hybrid fractional error function (HYBRID)	$\dfrac{100}{n-p} \displaystyle\sum_{i=1}^{n} \left[\dfrac{(q_{e\,exp} - q_{e\,cal})^2}{q_{e\,exp}} \right]_i$	[24]

where *n* is the number of data points, *p* is the number of parameters within the equation,$q_{exp}(mg.g^{-1})$ is the equilibrium value obtained from experiment and $q_{cal}\,(mg.g^{-1})$ is the calculated value using isotherm model.

_____

Sum of normalized errors (SNE)

Since each error criteria is likely to produce different sets of parameters of the isotherm, a standard procedure called *"Sum of the Normalized Errors"* is adopted to normalize and to combine the error in order to make a better and meaningful comparison between the parameter sets. It has been used to determine the best fitting isotherm equation by several investigations[**23,27–29**]. The calculation process for the *"Sum of the Normalized Errors"* is made as follows:

− Selection of an isotherm model and error function, and determination of the adjustable parameters which minimize the error function.
− Determination of the values for all other error functions for that isotherm parameter set.
− Computation of the other parameter sets associated with their error function values.
− Normalization and selection of the maximum parameter sets with respect to the largest error measurement.
− Summation of all these normalized errors for each parameter set.

RESULTS AND DISCUSSION

Characterization of materials

The chemical composition of the NIC was determined by X-ray Fluorescence (XRF) analysis. It shows that silica and alumina form the major composition (SiO_2 (61.7%), Al_2O_3 (24.2%)), while other mineral elements are present in minute amount as impurities (K_2O (3.28.%), MgO (1.55%), Fe_2O_3 (2.62%), Na_2O (0.513%), CaO (0.558%)).

The XRD patterns of the clay sample before and after adsorption are shown in **Figure 2**. The basalt distances (d-spacing [Å]) of predominant peaks found in the crude clay (**Figure 2 a**) indicate that the Natural Illitic Clay (NIC) was mainly composed of Illite associated with Quartz and Kaolinite. The XRD patterns before and after adsorption did not change at all, which indicating that the crystalline structure of the NIC was not changed after adsorption of CV, suggesting that the adsorption took place mainly on the external surface of NIC [**30**].
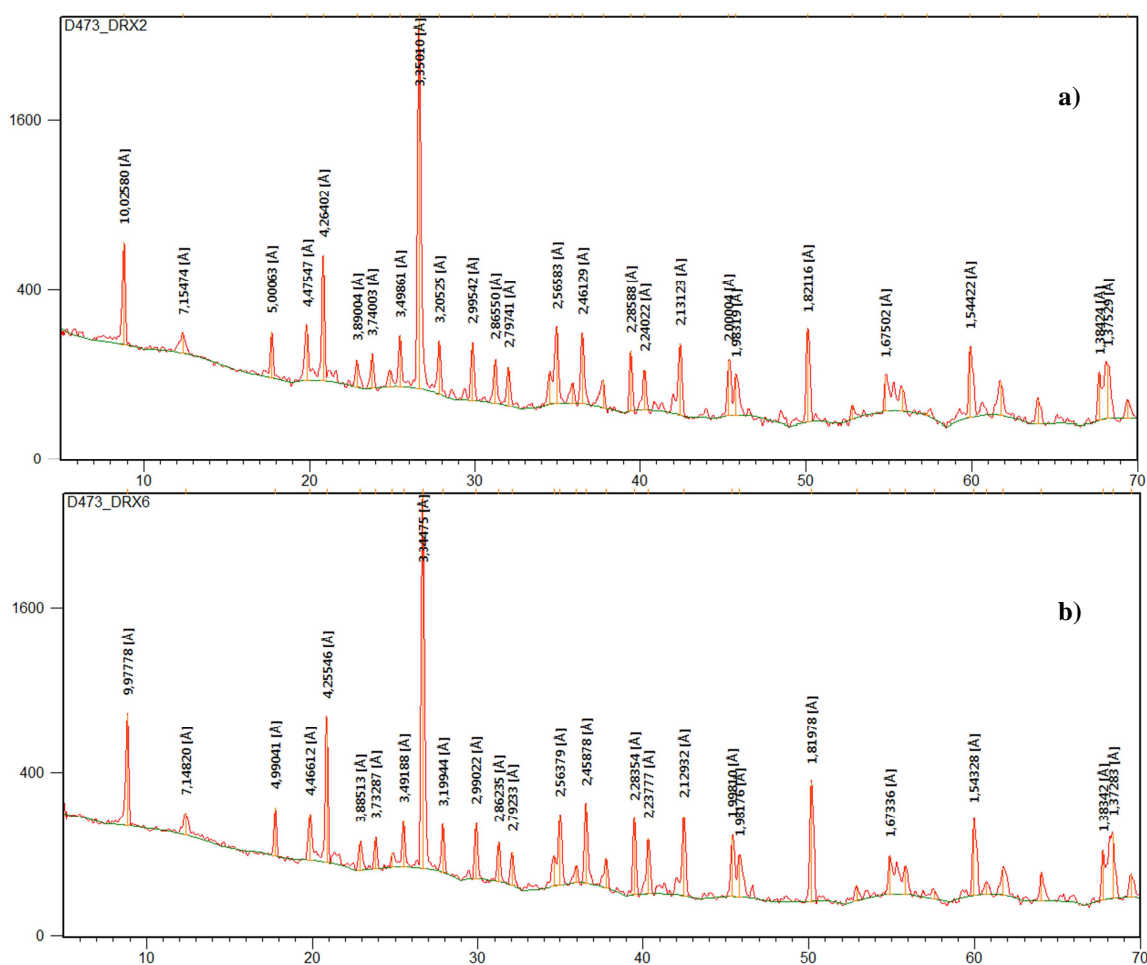

Figure 2: The XRD patterns of NIC a) before and b) after adsorption of CV

The Fourier transform infrared spectroscopy (FTIR) was used to determine the functional groups of the sample clay before and after adsorption of CV, and the results are shown in **Figure 3**. The interpretation of the bands follow those cited in literature[31]. Several bands were observed in the spectra of NIC. Before adsorption, the strong bands at *3698.5 cm^{-1}* and *3621.1 cm^{-1}* can be attributed to inner *OH* stretching vibration. The band at *3435.3 cm^{-1}*corresponds to the *OH* stretching of water adsorbed. The band at *913.5 cm^{-1}* is assigned to the existence of vibration of *Al-OH*. *Si-O* bending was observed at *1030.3 cm^{-1}*, while the *Si-O* stretching vibration was observed at *796.9* and at *694.2 cm^{-1}*, which reveal the presence of quartz in the NIC. After adsorption, the band's positions for these liaisons had not distinctly shifted. This can indicates that the affinity on CV to NIC surface can be attributed to the attractive Coulombic and van derWaals' forces[30].
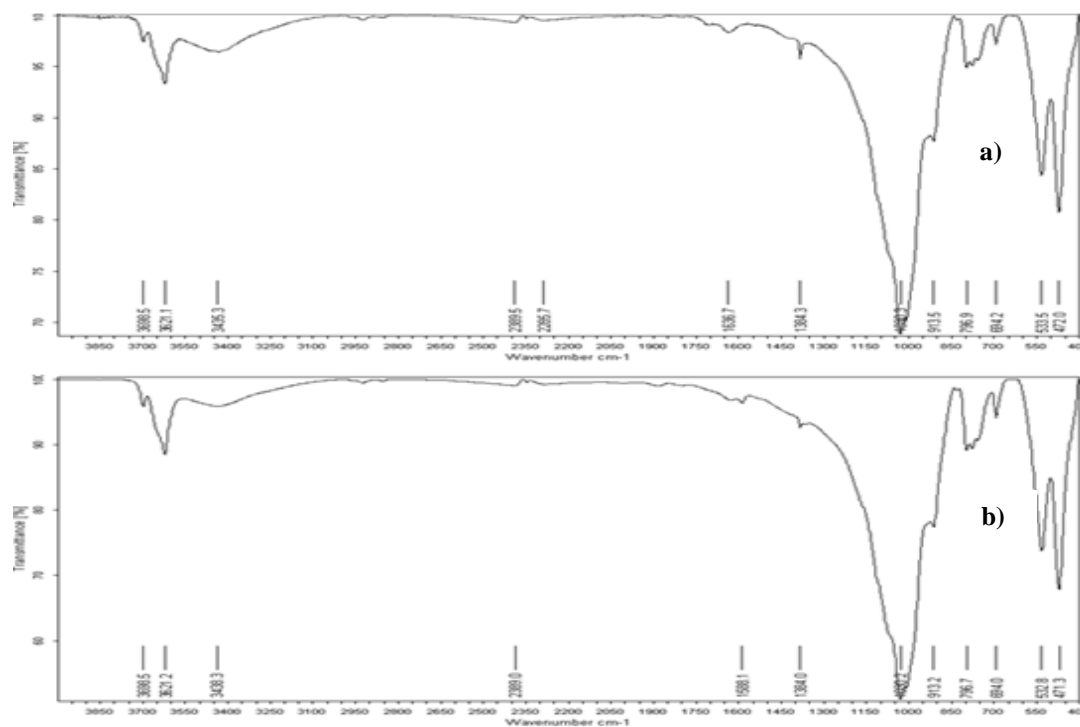

Figure 3:The FTIR patterns of NIC a) before and b) after adsorption of CV

Effect of initial dye concentration
The effect of initial CV concentration was investigated in a range of CV concentration varied from *5* to *30mg.L^{1}*, under operating conditions of *60min* as agitation time, *20mg* of NIC/*20mL* of CV solution, and solution PH was kept constant (at natural solution PH). The amount of CV dye adsorbed, Q_e, for different initial CV concentrations, C_i, onto the NIC is shown in **Figure 4**. The curve shows that the amount of CV dye adsorbed onto the NIC increases with increasing initial CV concentration. In high concentration, the adsorbed amount Q_e was higher, due probably to the larger driving force for mass transfer at higher concentrations[32].
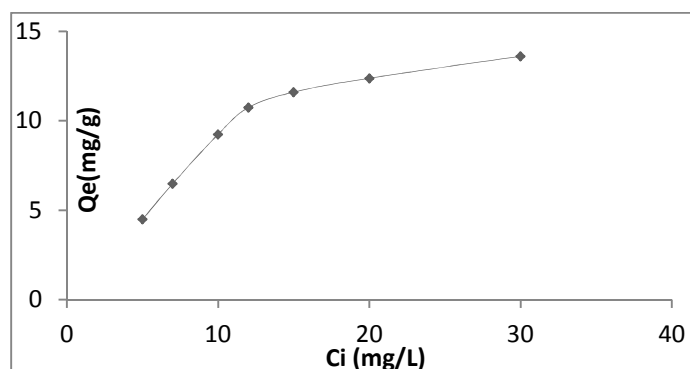

Figure 4: The variation the adsorbed amount, Q_e, with initial CV concentration C_i.

_____

Figure 5 shows the variation of removal percent of CV dye against initial CV concentration. It is clear that about *90%* of CV was removed when CV concentration was varied from *5* to *12mg.L^{-1}*, then, the CV removal percent decreases to about *45%* when CV concentration was *30mg.L^{-1}*. This decrease can be explained by the fact that an increase in CV concentration makes a high ratio of the number of CV ions present in solution to the number of available sites [**33**].
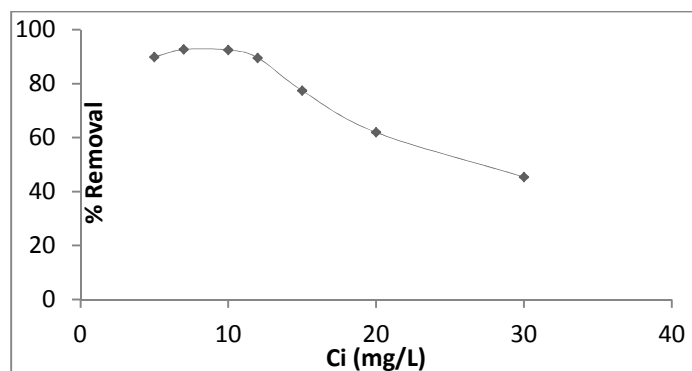

Figure 5: The effect of initial CV concentration on removal percent of CV by NIC

Determination of isotherm parameters sets
The adsorption isotherm is a basic requirement for the design of adsorption system. The best and the precise description of adsorption isotherm are important for prediction of adsorption parameters. In this work, the adsorption isotherm data for different initial dye concentrations were obtained by the dye concentration measurements after *NIC/CV* contact periods equal to the equilibrium time (*60min*), and were investigated.**Figure 6** shows the amount of CV adsorbed onto the solid phase (NIC), Q_e *(mg.g^{-1})*, against CV liquid phase concentration at equilibrium, C_e *(mg .L^{-1})*. The results show that the isotherms obtained display a *L*-type shape according to the Giles & al.[34] classification, which indicates the existence of a high affinity between the clay sample and the dye molecule.
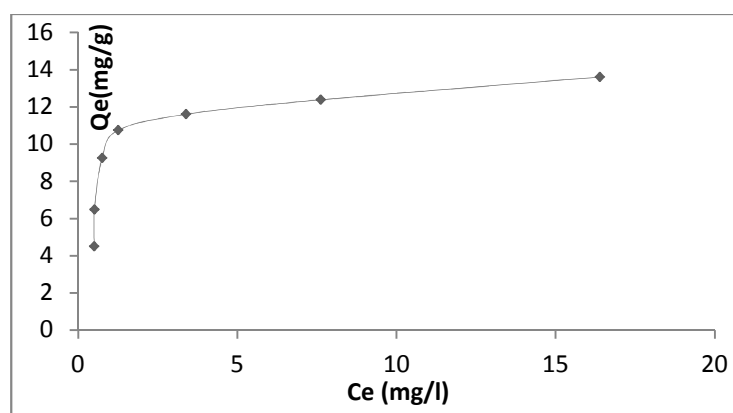

Figure 6: The adsorption isotherm of CV by NIC

In order to investigate and to model and quantify the affinity of CV for the NIC, eight different adsorption isotherm models (i.e. Langmuir, Freundlich, Dubinin–Radushkevich (D-R), Temkin, Redlich-Peterson, Sips, Khan and Toth) have been applied using nonlinear regression method. Five error functions detailed above were applied by using a trial and error procedure to fit the data and to determine the isotherm parameters, through the application of the *SOLVER ADD-IN* with Microsoft's spread sheet. The SNE values were used to evaluate the best error function for selecting the best isotherm model and the calculated isotherm parameters[**23,27,29**].

Table 4a-bsummarize the fitting parameters of the isotherm models used in this study, and the error function values. The figures in underlined type indicate the minimum values of *SNE* for an appropriate error function. As can be seen from **Table 4a-b**, it was found that the *SSE* function provides the best estimation of parameters for all isotherm models that have been examined in this study. The best estimation is due to the low value of *SNE* in 6 out of 8 systems (examining eight isotherm models) for all parameters isotherms examined. According to this argument, the *SSE* function was selected as the like error function for determination and examination of the best fit isotherm models to the experimental data. The isotherm models were evaluated using *SSE* function, and the values of parameters for each model are illustrated in **Table 5**. On the basis of *SSE* error value, the Sips isotherm model has

_____

the best performance for modeling the experimental data, with a lowest *SSE* error value, and the Freundlich isotherm model has a worst fitting degree with experimental data (*SSE =4.179612131* and*SSE =16.17560455* for the Sips and for the Freundlich isotherm models, respectively). On the basis of *SSE* error function, the experimental data and the predicted equilibrium curves using the non-linear regression method for the two and three parameter isotherms used in this study were showed in **Figure7**. As a show from **Figure 7**, the Sips isotherm model is the best fitting isotherm model for adsorption of CV onto NIC.

In general, the adsorption isotherm is characterized by the isotherm parameters whose values express the surface properties and the affinity of the adsorbate to adsorbent. The isotherm parameters obtained by nonlinear regression are listed in **Table 5**. The Sips isotherm model is found best to represent the equilibrium data with SSE value of *4.179612131*. According to the Sips isotherm model, the adsorption capacity value of CV onto NIC was *12.54051667mg.g^{-1}*. This value is near to the Q_{max}values determined by D-R and Toth isotherm models (Q_{max}=*12.46068666 mg.g^{-1}*andQ_t= *12.55048921 mg.g^{-1}*for D-Rand Toth isotherm models respectively). The Sips exponent *1/n* value is not close to unity (*1/n= 2.566247674*). It means that CV adsorption data for NIC has not exhibited Langmuir behavior, which indicates that the uptake was occurred on heterogeneous surface. This can be confirmed by the Toth isotherm exponent *"t"* which is not nearly unity (*t =3.409394014*).

Table 4.a: The calculated values of isotherms parameters and error analysis (Two-parameter isotherm models)

	X^2	SSE	ARE	EABS	HYBRID
Freundlich					
K_f	8,434126027	8,365013699	7,505022863	9,583287178	8,434126053
1/n	0,198108205	0,19418324	0,218167585	0,12623482	0,198108204
X^2	2,004823514	2,016824656	2,700548994	2,807031801	2,004823514
SSE	16,32821453	16,17560455	20,6869998	24,81221512	16,32821456
ARE	18,08670297	17,70422255	16,70077267	20,50235006	18,08670304
EABS	9,131848112	8,843535363	9,735249911	7,960900358	9,131848121
HYBRID	40,09647028	40,33649313	54,01097987	56,14063602	40,09647028
SNE	3,906697048	**3,860826436**	4,572452404	4,817739702	3,906697054
Langmuir					
Q_{max}	14,04898363	13,91279169	13,51531568	13,50042038	14,04898376
K_L	1,704150109	1,744001067	1,792531994	1,806630382	1,704150089
X^2	1,040704309	1,043278012	1,096419961	1,09588232	1,040704309
SSE	7,814300431	7,780799932	8,200169898	8,198875593	7,814300497
ARE	11,43384914	11,46322622	11,11364253	11,11415773	11,43384923
EABS	5,677911168	5,671747877	5,571494139	5,555542547	5,677911199
HYBRID	20,81408618	20,86556024	21,92839922	21,91764641	20,81408618
SNE	**4,848749039**	4,850835675	4,95076161	4,946858583	4,84874906
D-R					
Q_{max}	12,4900778	12,46068666	12,43872365	12,43872365	12,49006998
B_D	0,037373127	0,037715784	0,048126589	0,048126589	0,037373179
X^2	0,599712324	0,601357323	1,317305612	1,317305612	0,599712324
SSE	4,838855418	4,826628771	8,123400947	8,123400947	4,838850295
ARE	9,627038758	9,562475005	9,332907722	9,332907722	9,627022493
EABS	5,288009638	5,27126502	5,778757675	5,778757675	5,288003063
HYBRID	11,99424648	12,02714646	26,34611224	26,34611224	11,99424648
SNE	3,421259489	**3,412647779**	4,969447403	4,969447403	3,421256031
Temkin					
B	2,228220751	2,13316991	2,18847178	2,183748448	2,228186386
K_t	44,08624458	50,89783292	37,6341109	38,09751873	44,08886737
X^2	1,629449744	1,643811906	1,840289099	1,834091948	1,629449744
SSE	13,06654014	12,86870298	14,06163182	14,01944021	13,06643254
ARE	15,66426354	15,45276607	13,96740023	13,95745367	15,66426274
EABS	8,214076654	7,940863043	7,644444243	7,624026749	8,213999629
HYBRID	32,58899487	32,87623813	36,80578197	36,68183897	32,58899488
SNE	4,700096346	**4,654872108**	4,82232464	4,809468533	4,700079266

_____

Table 4.b: The calculated values of isotherms parameters and error analysis (Three-parameter isotherm models)

	X^2	SSE	ARE	EABS	HYBRID
R-P					
A	19,22858242	20,78269688	20,86763105	20,86763105	19,22833563
B	1,123423041	1,316490693	1,332801719	1,332801719	1,123391563
g	1,085110317	1,053747632	1,075591694	1,075591694	1,085114039
X^2	0,960372517	0,972905514	1,082743832	1,082743832	0,96037252
SSE	7,565709229	7,423030541	8,616693848	8,616693848	7,565774844
ARE	11,82808297	11,52706755	11,39518848	11,39518848	11,82814983
EABS	6,373420203	6,030076915	5,979229133	5,979229133	6,373486019
HYBRID	24,00931292	24,32263786	27,06859581	27,06859581	24,00931299
SNE	4,651973995	**4,579246396**	4,901536775	4,901536775	4,651997594
Sips					
K_s	5,219559061	4,635235376	4,321351597	4,321351597	5,219406901
Q_s	12,50721435	12,54051667	12,38994835	12,38994835	12,50722348
1/n	2,743926335	2,566247674	2,965937278	2,965937278	2,7438854
X^2	0,520716578	0,524373153	1,096937772	1,096937772	0,520716579
SSE	4,212587611	4,179612131	6,99482991	6,99482991	4,212572175
ARE	8,898509366	8,979578457	8,545991821	8,545991821	8,898534159
EABS	4,925472468	4,935759278	5,320329931	5,320329931	4,925482656
HYBRID	13,01791446	13,10932882	27,4234443	27,4234443	13,01791446
SNE	**3,468398547**	3,481312812	4,951714144	4,951714144	3,468401017
Khan					
Q_{max}	1,056288057	1,090534354	0,796587219	0,799545788	1,045108156
b_k	35806,13355	36027,86809	34224,14052	34249,74965	37838,16832
a_k	0,801877906	0,805811399	0,785391643	0,780301437	0,801900095
X^2	2,004710825	2,01663762	2,767928948	2,170939928	2,00471668
SSE	16,3267183	16,17457786	21,24049425	17,24519934	16,32718511
ARE	18,08462502	17,70470859	16,78121957	16,79611951	18,08600896
EABS	9,131610424	8,844178915	9,777781432	9,183413177	9,131546193
HYBRID	50,11777062	50,41594049	69,19822369	54,27349821	50,117917
SNE	4,151025496	**4,102078101**	4,927856423	4,248433081	4,151121655
Toth					
Q_t	12,52224811	12,55048921	12,40625805	12,40625805	12,52224838
k_t	0,936863293	0,95084433	1,113018758	1,113018758	0,936865875
t	3,950309578	3,409394014	2,506580977	2,506580977	3,950292331
X^2	0,645240304	0,649714829	0,782364313	0,782364313	0,645240304
SSE	5,20163201	5,159516745	6,035695903	6,035695903	5,201631379
ARE	9,980962755	9,836655462	9,237325526	9,237325526	9,980958551
EABS	5,426854438	5,274827723	4,471220368	4,471220368	5,426843153
HYBRID	16,13100761	16,24287073	19,55910782	19,55910782	16,13100761
SNE	4,511273996	**4,47326273**	4,749400888	4,749400888	4,51127139

Table 5 :The SSE and values of parameters isotherm models

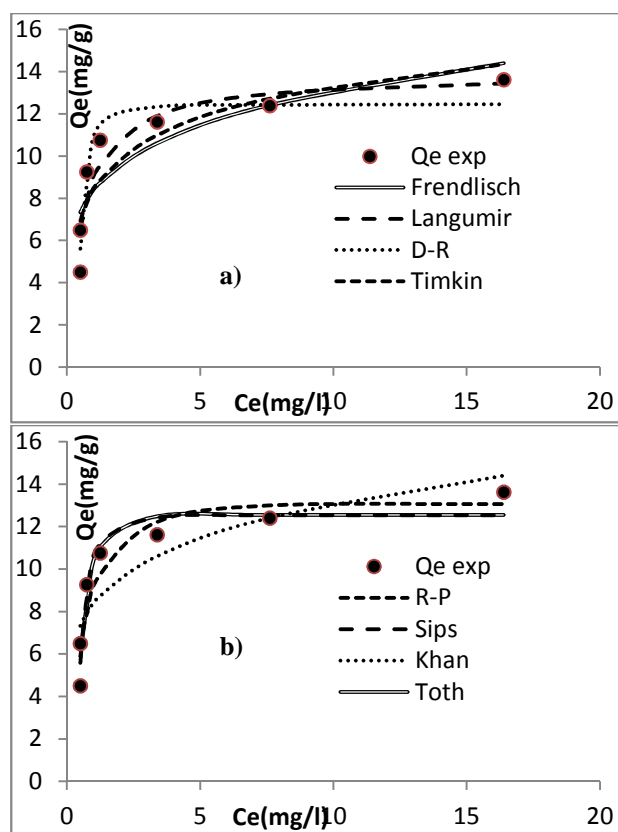| Parameters isotherm models			
Two-parameter Isotherm		***Three-parameter Isotherm***	
Parameter	***value***	***Parameter***	***value***
Freundlich		***R-P***	
K_f(l/mg)	8,365013699	A(L/g)	20,78269688
1/n	0,19418324	B(L/mg)	1,316490693
		g	1,053747632
SSE	16,17560455	SSE	7,423030541
Langmuir		***Sips***	
Q_{max}(mg/g)	13,91279169	Ks(L/mg)	4,635235376
K_L(l/mg)	1,744001067	Qs(mg/g)	12,54051667
		1/n	2,566247674
SSE	7,780799932	SSE	4,179612131
D-R		***Khan***	
Q_{max}(mg/g)	12,46068666	Q_{max}(mg/g)	1,090534354
B_D(kJ^2.mol^{-2})	0,037715784	b_k	36027,86809
		a_k	0,805811399
SSE	4,826628771	SSE	16,17457786
Temkin		***Toth***	
B	2,13316991	Q_t(mg/g)	12,55048921
K_T(L/g)	50,89783292	K_t	0,95084433
		t	3,409394014
SSE	12,86870298	SSE	5,159516745

_____

Figure 7:The comparison of isotherm models with experimental data: a) Two-parameter isotherm models. b) Three-parameter isotherm models

The essential feature of the Langmuir isotherm can be expressed by means of a dimensionless constant *"R_L"* that is referred to as separation factor. It is defined by the following relationship[**35**]:

$$R_L = \frac{1}{\left(1 + K_L C_i\right)}$$

Where K_L and $C_i (mg.L^{-1})$ are the Langmuir constant and the initial dye concentration respectively. As the *"R_L"* value lie between 0 and 1, the on-going adsorption process is favorable. The variation of *"R_L"* values for CV adsorption onto NIC with initial CV concentration is indicated in **Figure 8.** The *"R_L"* values for Crystal Violet adsorption onto NIC are between *0.01875468* and *0.1028806*, and therefore, its adsorption was favorable. This can also be concluded from the Frendlich model fitting results.
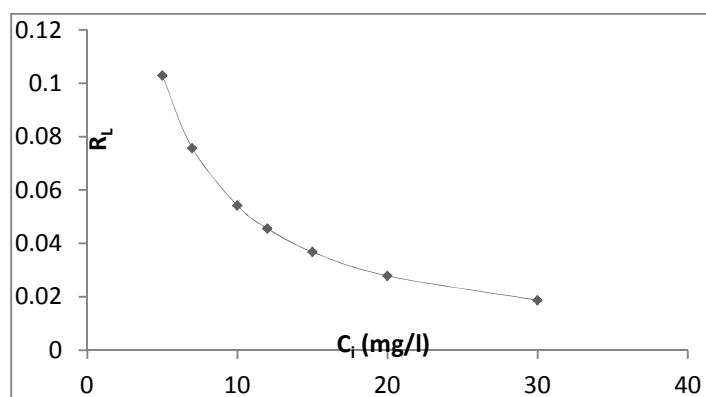

Figure 8: The variation of "R_L" values for CV adsorption onto NIC with initial CV concentration

The magnitude of the exponent *"1/n"* of Frendlich isotherm , gives an indication about the favorability of adsorption such that in favorable adsorption process, the value of *1/n* should be in the range of *0-1*[**35**]. In this study, the value

_____

of *1/n* is equal to *0.19418324* ,what indicates that the adsorption of CV onto NIC was favorable (**Table 5**). The Freundlich constant *"n"* is a measure of the deviation from linearity of the adsorption. Since the value of *"n"* is above unity (*n = 5.14977502*), the adsorption being favorable was of physical nature[**36**].

The constant *"b"*, related to the variation of adsorption energy concluded from Temkin isotherm, is positive. These indicate that the adsorption reaction was exothermic[**37**].The free energy *E* of CV adsorption onto NIC was considered via Dubinine-Radushkevich (D-R) model. It gives information about the adsorption mechanism, for example, if the magnitude of *E* is between *8* and *16 KJ.mol^{-1}*, the adsorption process that has taken place is of chemical type, and when *E < 8KJ/mol*, the adsorption process proceeds physically . As can be concluded from **Table 5**, this energy that is less than *8 kJ.mol^{-1}*(*E= 3.641023096KJ.mol^{-1}*), confirms that the adsorption process of CV onto NIC was controlled by physical adsorption process[**38**].

CONCLUSION

In this study, the adsorption of Crystal Violet (CV) by Natural Illitic Clay (NIC) was characterized using XRD and FTIR technics, and the adsorption data were explained by application the nonlinear regression method. The XRD analysis suggested that the adsorption was took place on the external surface of NIC. The FTIR concluded that the affinity on CV to NIC surface can be attributed to the weak liaison (i.e. Coulombic and van derWaals' forces). The adsorption isotherms were analyzed using eight different isotherm models and five different error functions. To select the best error function, the *SNE* procedure was used, and on the basis of *SNE* values, the *SSE* function was select as the best error function to choose the best isotherm model. It was found that the Sips isotherm model provided the best fit, and the adsorption capacity of the NIC was determined to be *12,54051667mg.g^{-1}*. Based on the obtained isotherms parameters values, it appears that the adsorption of CV onto NIC was favorable, and confirmed that this adsorption was controlled by physic-sorption.

REFERENCES

[1] Klimiuk, E.; Filipkowska, U.; Libecki, B. *Pol. J. Environ. Stud.,***1999**, *8*, 81–88.
[2] Snider, E. H.; Porter, J. J.;*J. Water Pollut. Control Fed.,***1974**, 886–894.
[3] Majewska-Nowak, K.; Kabsch-Korbutowicz, M.; Winnicki, T. *Desalination,***1997**, *108* (1), 221–229.
[4] Lin, S. H.; Peng, C. F.;*Water Res.,***1994**, *28* (2), 277–282.
[5] Zhu, H.; *Ind. Safety. Envir. Prot.*; 12, 16-18.*http://en.cnki.com.cn/Article_en/CJFDTOTAL-GYAF200712008.htm.*
[6] Yagub, M. T.; Sen, T. K.; Afroze, S.; Ang, H. M.;*Adv. Colloid Interface Sci.,***2014**, *209*, 172–184.
[7] Wang, L.; Zhang, J.; Zhao, R.; Li, C.; Li, Y.; Zhang, C.;*Desalination,***2010**, *254* (1), 68–74.
[8] Annadurai, G.; Ling, L. Y.; Lee, J.F.;*J. Hazard. Mater.,***2008**, *152* (1), 337–346.
[9] Weng, C.H.; Pan, Y.F.;*J. Hazard. Mater.,***2007**, *144* (1), 355–362.
[10] Gürses, A.; Doğar, Ç.; Yalçın, M.; Açıkyıldız, M.; Bayrak, R.; Karaca, S.;*J. Hazard. Mater.,***2006**, *131* (1), 217–228.
[11] Mouzdahir, Y. El; Elmchaouri, A.; Mahboub, R.; Gil, A.; Korili, S. A.;*Desalination,***2010**, *250* (1), 335–338.
[12] Langmuir, I.;*J. Am. Chem. Soc.,***1918**, *40* (9), 1361–1403.
[13] Freundlich, H.M.F.;*Journal of Physical Chemistry.,***1906**, 385–370.
[14] Dubinin, M. M.;*Chem. Rev.,***1960**, *60* (2), 235–241.
[15] Temkin, M. I.; Pyzhev, V.;*Acta Physiochim URSS,***1940**, *12* (3), 217–222.
[16] Redlich, O.; Peterson, D. L.;*J. Phys. Chem.,***1959**, *63* (6), 1024–1024.
[17] Sips, R. *J.*; *Chem. Phys.,***1948**, *16* (5), 490–495.
[18] Khan, A. R.; Ataullah, R.; Al-Haddad, A.;*J. Colloid Interface Sci.,***1997**, *194* (1), 154–165.
[19] Toth, J.;*Acta Chim Acad Sci Hung.,***1971**, *69* (3), 311–328.
[20] Kumar, K. V.; Sivanesan, S.;*J. Hazard. Mater.,***2006**, *134* (1–3), 277–279.
[21] Kumar, K. V.;*Dyes Pigments,***2007**, *74* (3), 595–597.
[22] Ho, Y.-S.;*Carbon,***2004**, *42* (10), 2115–2116.
[23] Anirudhan, T. S.; Radhakrishnan, P. G.;*Desalination,***2009**, *249* (3), 1298–1307.
[24] Ng, J. C. Y.; Cheung, W. H.; McKay, G.;*J. Colloid Interface Sci.,***2002**, *255* (1), 64–74.
[25] Mittal, A.; Mittal, J.; Malviya, A.; Kaur, D.; Gupta, V. K.;*J. Colloid Interface Sci.,***2010**, *343* (2), 463–473.
[26] Brdar, M.; Šćiban, M.; Takači, A.; Došenović, T.;*Chem. Eng. J.,***2012**, *183*, 108–111.
[27] Gunay, A.;*J. Hazard. Mater.*, **2007**, *148* (3), 708–713.
[28] Kundu, S.; Gupta, A. K.;*Chem. Eng. J.,***2006**, *122* (1), 93–106.
[29] Chan, L. S.; Cheung, W. H.; Allen, S. J.; McKay, G.;*Chin. J. Chem. Eng.,***2012**, *20* (3), 535–542.
[30] Zhang, X.; Hong, H.; Li, Z.; Guan, J.; Schulz, L.;*J. Hazard. Mater.,***2009**, *170* (2–3), 1064–1069.
[31] Madejova, J.; Komadel, P.;*Clays Clay Miner.,***2001**, *49* (5), 410–432.

---

[32] Tehrani-Bagha, A. R.; Nikkar, H.; Mahmoodi, N. M.; Markazi, M.; Menger, F. M.;*Desalination,***2011**, *266* (1), 274–280.

[33] Al-Shahrani, S. S.;*Alex. Eng. J.,***2014**, *53* (1), 205–211.

[34] Giles, C. H.; Smith, D.; Huitson, A.;*J. Colloid Interface Sci.,***1974**, *47* (3), 755–765.

[35] Ozdes, D.; Duran, C.; Senturk, H. B.; Avan, H.; Bicer, B.;*Desalination Water Treat.,***2014**, *52* (1-3), 208–218.

[36] Özcan, A. S.; Erdem, B.; Özcan, A.;*Colloids Surf. Physicochem. Eng. Asp.,***2005**, *266* (1), 73–81.

[37] Hadi, M.; Samarghandi, M. R.; McKay, G.;*Chem. Eng. J.,***2010**, *160* (2), 408–416.

[38] Helfferich, F. G.;*Ion exchange*; Courier Corporation, **1962**.